

# Nacelle Actuation System with Linear Electric Motor

Krzysztof Falkowski, Maciej Henzel

Military University of Technology, Warsaw, Poland

**Abstract:** This paper presents the results of research work on the construction of nacelle actuator with linear tubular electrical motor. The laboratory model was designed at the Military University of Technology. It was verified by finite element method. The test provided information for dynamic simulation and it can be used to verification of linear tubular motor construction.

**Keywords:** actuator, linear motor, magnets

The modern aircraft need digital active control system to stabilization angular orientation in the air space and control the trajectory of flight. The aircraft are designed as more electric. Now, the hydraulic and pneumatic systems are replaced by electromechanical units. The electrohydraulic actuators are replaced by electromechanical actuators with linear tubular electric motor. This kind of actuator assures high reliability, good dynamic property and strong thrust forces.

## 1. Introduction

The aircraft use the different types of actuators. They work as convertors of electric energy for mechanical energy. These elements are used as direct elements for adjust weapons and boarding equipment (e.g. for open loading ram) and flight control system of aircraft. Hydraulic actuators have been dominant in the past years. They assure strong forces and have good proportion between mass and energy.

The aircraft are equipped in flight control system after the Second World War. This system has supported pilots during flight. Frequently, aircraft has got mixed actuators system. The electromechanical actuators are used as preamplifiers. They change electrical control signal for move thrust tube of actuator. The electromechanical actuator moves a selector valve of hydraulic cylinder and a piston of hydraulic cylinder changes a control surface of aircraft. The hydraulic actuator works as a power amplifier. Now, the mixed systems are exchanged by electrohydraulic actuator. The preliminary amplifier and the power amplifier are made in one unit. There is an electrical control signal and generates strong forces by piston of fluid actuator.

Recently, aircraft has been designing in the technology under the More Electric Aircraft (MEA) concepts. This technology make an assumption of the use more electrical elements in onboard systems to reduce weight of the pneumatic and hydraulic piping, easier maintainability and finally is enhanced safety of the flight. In practical application MEA technology was implemented in the

modern military and commercial aircraft such as the Airbus A380, Boeing 787, F-16 Falcon.

The electrohydraulic actuators are replaced by electromechanical actuators in modern aircraft. Especially, modern linear electric motor can be used a nacelle actuators. This type of actuator has got a bandwidth. The classical actuators use the screw to change a rotation move in the linear move. There is a gear to reduce a speed of electric drive. All these elements are eliminated in the linear tubular motor. This actuator assures good dynamic and static parameters and reliability. The modern military aircraft and unmanned aerial vehicles (UAVs) must be equipped in high speed and reliability actuators. This paper presents the results of investigations of the aircraft's actuator with linear tubular electrical motor.

## 2. Construction on linear actuator

The electromechanical actuators use additional element exchanged rotation to linear movement. The linear actuator transforms electric energy to linear move of thrust tube. The linear electric motor is divided in two flat and tubular. The tubular linear motors have got runner shaped as a pipe (fig. 3).

The linear motor is similar to classical rotation motor (fig. 1). If we cut the rotor of electrical motor at long radial surface and flatten it is a flat runner of linear motor (fig. 2). If the flat runner of motor rolls around their longitudinal axis it is a tubular runner of linear rotor (fig. 3).

The tubular linear motors divided in two slotted and slotless armature. This divide appears from construction of armature. Next divide appears from runner construction. There are runners with surface mounted magnets and interior mounted magnets.



Fig. 1. The view of rotor of rotation drive

Rys. 1. Widok wirnika silnika obrotowego



**Fig. 2.** The view of runner of flat linear drive  
**Rys. 2.** Widok biegnika liniowego silnika płaskiego



**Fig. 3.** The view of runner of tubular linear drive  
**Rys. 3.** Widok biegnika liniowego silnika tubowego

The electrical linear drive with interior mounted magnets is the most popular construction. There can be used ring shaped magnets with axial orientation of magnetization. This construction assures high thrust forces. The runner blocks after power off, because the magnetic field of magnets generated strong radial magnetic force and the rotor does not move (fig. 4). The armature of slotted linear motor is made of soft iron and magnets generate attractive magnetic force (fig. 4). Sometimes, this performance is disadvantage in practical applications. This disadvantage removes in the slotless linear motor (fig. 5). There is no armature.

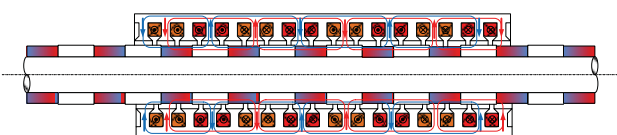


**Fig. 4.** The linear tubular slotted electrical motor with interior mounted magnets  
**Rys. 4.** Tubowy silnik liniowy ze żłobkami z magnesami montowanymi wewnątrz

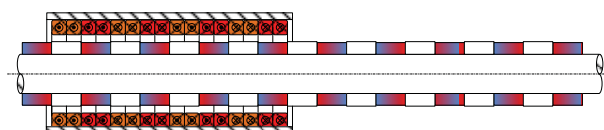


**Fig. 5.** The linear tubular slotless motor with interior mounted magnets  
**Rys. 5.** Tubowy silnik liniowy bezżłobkowy z magnesami montowanymi wewnątrz

The slotted linear motor with interior mounted magnets was selected as a source of thrust force in the electromechanical actuator. Figure 6 presents the main geometric relation in the linear motor.

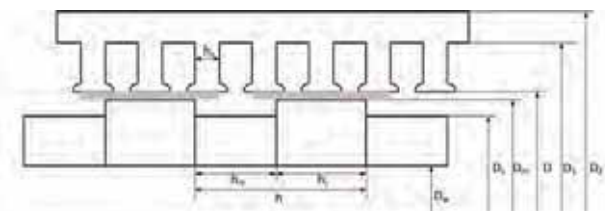


**Fig. 6.** Geometrical relation in the linear motor with interior magnets  
**Rys. 6.** Zależności geometryczne w silniku liniowym z wewnątrz zamontowanymi magnesami

The main parameter of rotor is synchronous speed. This parameter depends on pole pitch  $h$  and frequency of supply  $f$ . It is equal:

$$v = 2fh \quad (1)$$

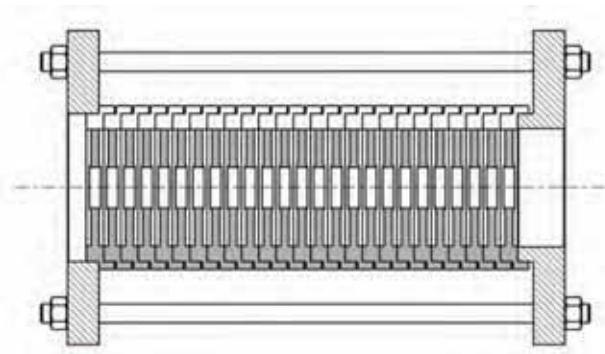


**Fig. 7.** The armature of linear motor with 12 poles  
**Rys. 7.** Stator silnika liniowego z 12 biegunami

### 3. Laboratory model of linear motor

The laboratory model of actuator with tubular linear motor was made for tests. The armature of motor was made from Armco soft iron. It consists from the modules. The winding of rotor was located between two modules. Authors made two armatures with 24 and 12 poles (fig. 7). Figure 8 shows a module of a stator while figure 9 presents a stator for 12 poles. The winding was connected outside the stator. There can be joined end of wire in star or triangle configuration.



**Fig. 8.** The single element of armature of linear motor  
**Rys. 8.** Element statora silnika liniowego



Fig. 9. The armature of linear drive

Rys. 9. Stator silnika liniowego

In the picture the runner of motor is shown. There is an alumina rod with screwed of end. On the rod is mounted ferromagnetic core (armco soft iron) and magnets. There is retained configuration of vector of magnetization (figs. 10–11).

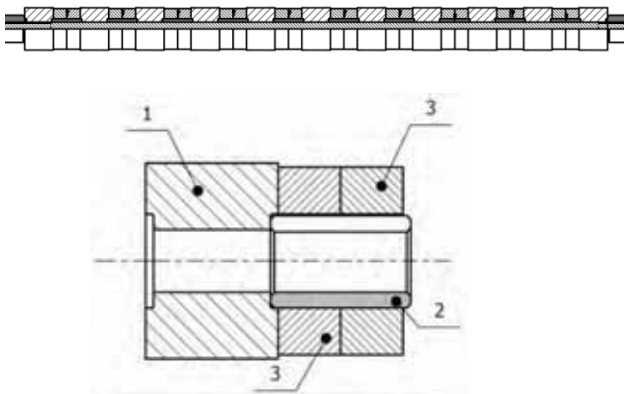


Fig. 10. The runner with interior mounted magnets: soft iron core (1), magnets (3) and cooper spring ring (2)

Rys. 10. Biegnik silnika z wewnątrz montowanymi magnesami: żelazo miękkie (1), magnes (3), miedziany pierścień (2)

#### 4. The FEM model of linear actuator with tubular electric drive

FEM models were made for tested magnetic field of runner, inductance for different current in the coil and frequency. The results of tests provide information about a construction and parameters for simulation in MATLAB/Simulink.

The first test verified the magnetization in the runner. The geometry of rotor are shown in fig. 11. This model has got five regions: air, cooper – spring rings, alumina – rod, magnets and soft iron. The axisymmetric model was used to tested simulation.

The magnetization and magnetic flux density were obtained for the runner. The magnetization of magnet is presented in fig. 12. The blue color shows negative direction of magnetization and positive direction shows red color. There result for  $O_z$  direction is presented. All the figures are presented results in the cylindrically coordinate.

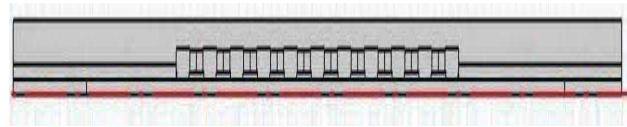


Fig. 11. Geometry of linear drive runner

Rys. 11. Geometria biegnika silnika liniowego

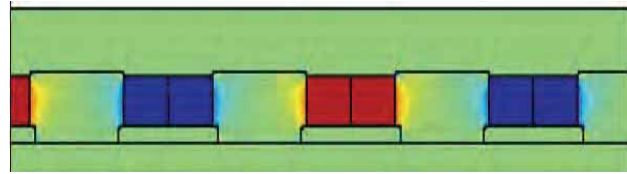


Fig. 12. The magnetization of magnet

Rys. 12. Wektor magnetyzacji magnesów

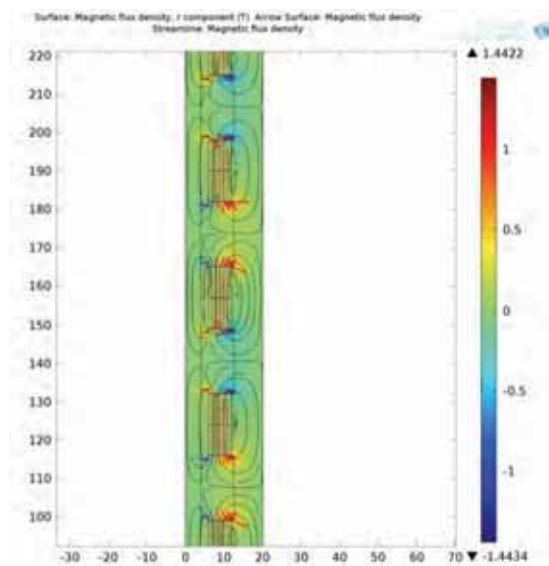


Fig. 13. The magnetic flux density in the runner – component  $B_r$

Rys. 13. Indukcja magnetyczna w biegniku – składowa  $B_r$

Figure 13 presents the magnetic flux density in the runner. Arrows present direction of magnetic flux density. This result will be used to verification construction. Figure 14 shows distribution of magnetic flux density on the surface of runner ( $r = 12.5$  mm). Next lines show the distribution over surface of runner. The difference between  $r = 12.5$  mm and line equals distance between surface of runner and surface of measurement.

The results presented in fig. 12–14 were used to verification runner of linear tubular drive.

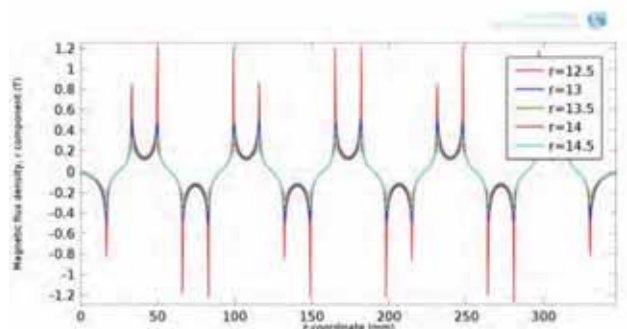


Fig. 14. The magnetic flux density under surface of runner

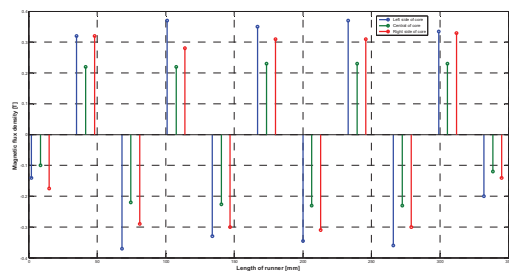
Rys. 14. Indukcja magnetyczna nad powierzchnią wirnika



**Fig. 15.** The runner with interior mounted magnets  
**Rys. 15.** Biegnik z wewnątrz montowanymi magnesami



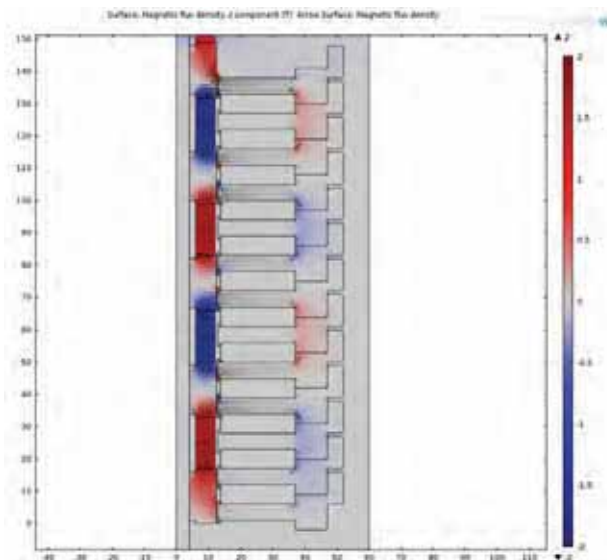
**Fig. 16.** The measurement of magnetic flux density  
**Rys. 16.** Pomiar indukcji magnetycznej



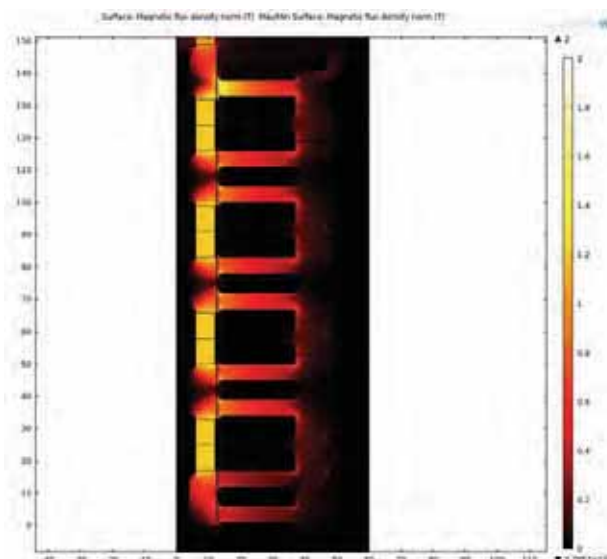
**Fig. 17.** The characteristic of magnetic flux density  
**Rys. 17.** Charakterystyka indukcji magnetycznej

Figure 16 shows the runner and the measurement of magnetic flux density by gaussmeter LakeShore 460 (fig. 17).

The next was tested the distribution of magnetic flux density in a magnetic circuit of linear motor. This test provides information about magnetic flux density in the air gap. Figure 18 presents component  $B_z$  of vector magnetic flux density. The component  $B_r$  (radial) magnetic flux density is shown in fig. 20. These pictures are presented the section by the runner and armature. Figure 18 presents a module of magnetic flux density. All tests were made for the axisymmetric model.



**Fig. 18.** Component  $B_z$  of magnetic flux density  
**Rys. 18.** Składowa  $B_z$  indukcji magnetycznej



**Fig. 19.** Module of magnetic flux density  
**Rys. 19.** Moduł indukcji magnetycznej

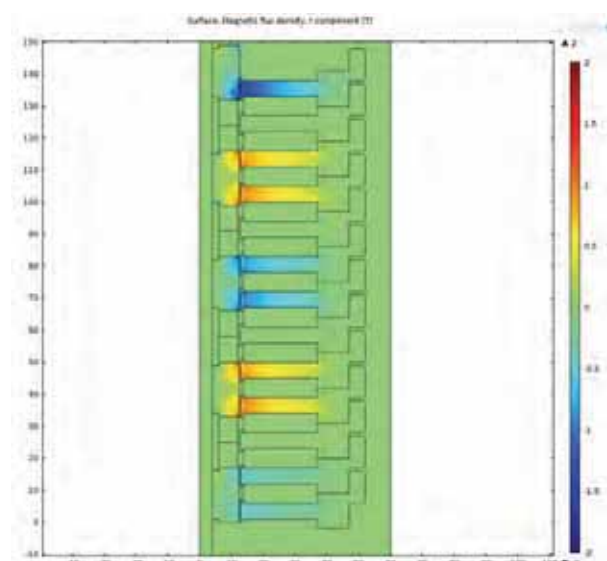


**Fig. 20.** Component  $B_r$  of magnetic flux density  
**Rys. 20.** Składowa  $B_r$  indukcji magnetycznej

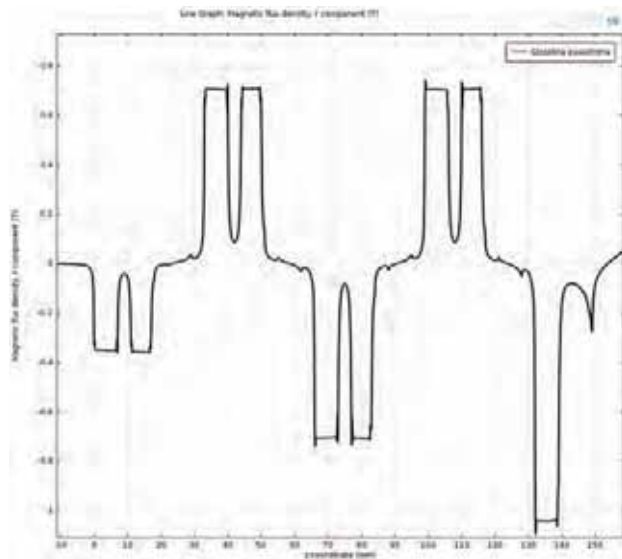


**Fig. 21.** Magnetic flux density in the air gap  
**Rys. 21.** Indukcja magnetyczna w szczelinie powietrznej

The results can be used to identification magnetic flux density in the air gap generated by magnets. This flux is necessary to use dynamic simulation of linear motor. Figure 21 shows the magnetic flux density in the air gap. We assume, that the magnetic flux has got the same value in the air gap. The experimental calculates this characteristic is very difficult. We can only measure magnetic flux in the air gap for the end of armature. The air gap is about 0.25 mm and the flex probe has got dimension 0.2 mm and we can penetrate only 20 mm.

In fig. 21 we can see the extreme effect. When the rotor has got end, the magnetic field is smaller than central part of rotor. The flux in the central part of rotor is good because magnets mount in the rotor supply the core from two directions.

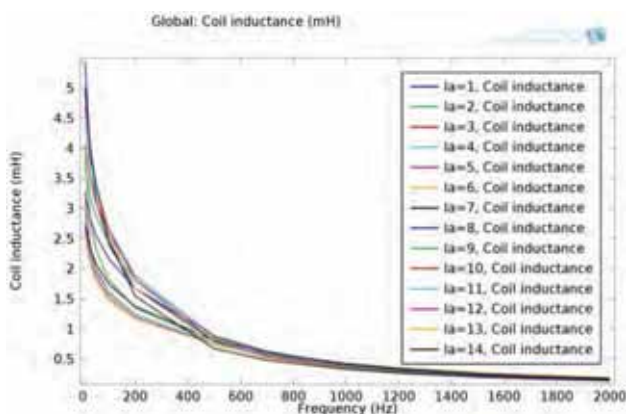


**Fig. 22.** Characteristic of inductance coil  $N_a$   
**Rys. 22.** Charakterystyka indukcyjności cewki  $N_a$

Last tooth of armature can saturated because the strong magnetic field generated by two magnets are supplied one tooth.

The last test was used to estimated inductance of coil of magnets. This parameter we need for obtain the matrix of impedances of electrical part of motor. The result of measurement is presented in fig. 22–24.

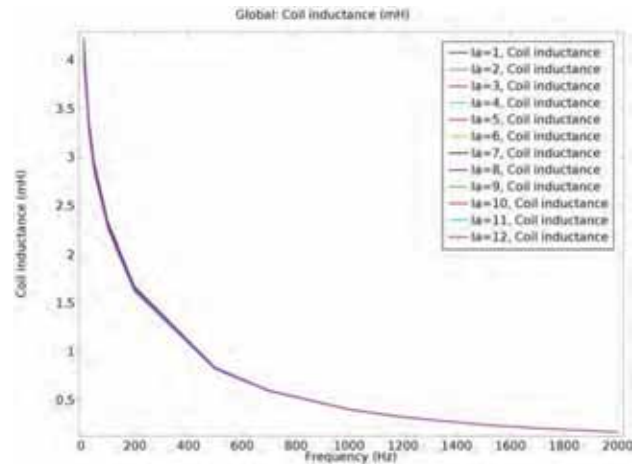


**Fig. 23.** Characteristic of inductance coil  $N_b$   
**Rys. 23.** Charakterystyka indukcyjności cewki  $N_b$

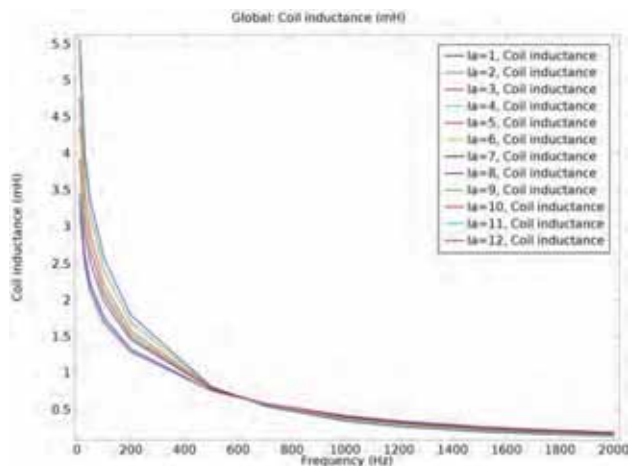


**Fig. 24.** Characteristic of inductance coil  $N_c$   
**Rys. 24.** Charakterystyka indukcyjności cewki  $N_c$

## 5. Summary

There results of actuator with linear motor investigation are presented. This construction has got a lot of advantages then classical electromechanical actuators.

The finite elements method was used to verificate construction of designed linear motor.

The results of simulation were made use of mathematical model of linear tubular motor. This model was made in the MATLAB-Simulink. The control was tested in the MATLAB and there was optimized control law and control algorithm.

The finite element method allows estimate parameter of motor without physical model, which is winding in the factory. This methodology allows for continuation investigations.

## Acknowledgements

The work was financed in part from the government support of scientific research for years 2010–2013, under grant No. O N509 165238. The work was also supported by Innovative Economy Programme, No. POIG.02.02.00-14-022/09.

## References

1. Bianchi N., Bolognami S., Corda J., *Tubular linear motors: A Comparison of Brushless PM AN SR Motors*, Power Electronics, Machines and Drivers, 2002.
2. Bianchi N., Bolognami S., Corte D., Tonel F., *Tubular linear permanent magnet motors: an overall comparison*, IEEE Transactions on Industry Application, Vol. 39, No. 2, 2003.
3. Bianchi N., Dai Pre M., Bolognami S., *Design of fault-tolerant IPM motor for electric power steering*, IEEE Transactions on Vehicular Technology, Vol. 55, No. 4, 2006
4. Bianchi N., *Analytical field computation of a tubular permanent – magnet linear motor*, IEEE Transactions on Magnetics, Vol. 36, No. 5, 2000.
5. Luis R., Quadrado J.C., *On PM tubular linear synchronous motor modeling*. ■

### Lotniczy układ wykonawczy z silnikiem liniowym

**Streszczenie:** W artykule przedstawione zostały wyniki prac prowadzonych nad opracowaniem lotniczego układu wykonawczego z tubowym liniowym silnikiem elektrycznym. Model taki został zaprojektowany w Wojskowej Akademii Technicznej. Wyniki przeprowadzonych testów umożliwiły wyznaczenie parametrów do symulacji dynamicznych i weryfikacji konstrukcji tubowego silnika liniowego.

**Słowa kluczowe:** układ wykonawczy, silnik liniowy, magnes

#### Krzysztof Falkowski, PhD

Krzysztof Falkowski graduated Military University of Technology. He received PhD title in 1999. He does research about magnetic suspensions, magnetic bearings and bearingless electric motors. He is author or co-author of many articles about magnetic levitation phenomena. He is organizer of Magnetic Suspension Workroom of Aircraft Engines Laboratory in Military University of Technology.

*e-mail:* krzysztof.falkowski@wat.edu.pl



#### Maciej Henzel, PhD Eng

Maciej Henzel graduated of Military University of Technology. He received PhD title in mechanics discipline and control systems specialization in 2004. He works in Military University of Technology since 1998. He does research aircraft control and actuation systems, measurement systems and bearingless machines. He is author or co-author of many articles about new trends in on-board systems, modern control methods and bearingless drives.

*e-mail:* maciej.henzel@wat.edu.pl

